PAVELČÍK, F. & SIVÝ, J. (1989). *XFPS89. A Computer Program for Automatic Structure Determination by Fourier, Patterson and Superposition Methods.* Komensky Univ., Bratislava, Czechoslovakia.
PAVELČÍK, F., SIVÝ, J., RIZZOLI, C. & ANDREETTI, G. D. (1992). *J. Appl. Cryst.* **25**, 328-329.
PAVELČÍK, F., ŽEMLIČKA, M., KETTMANN, V. & KRÄTSMÁR-ŠMOGROVIČ, J. (1987). *Chem. Pap.* **41**, 433-440.
RAMACHANDRAN, G. N. & SRINIVASAN, R. (1970). *Fourier Methods in Crystallography.* New York: Wiley-Interscience.
RIZZOLI, C. (1990). Unpublished.
SHELDRICK, G. M. (1982). Testing structures for direct methods. Univ. of Göttingen, Germany.
SHELDRICK, G. M. (1985). In *Crystallographic Computing* 3, edited by G. M. SHELDRICK, C. KRÜGER & R. GODDARD, pp. 175-189. Oxford Univ. Press.
SHELDRICK, G. M. (1986). *SHELXS86.* Program for the solution of crystal structures. Univ. of Göttingen, Germany.
SIVÝ, J., PAVELČÍK, F., KRÄTSMÁR-ŠMOGROVIČ, J., ŽEMLIČKA, M. & SERESSOVA, V. (1990). *Collect. Czech. Chem. Commun.* **55**, 2924-2932.
SIVÝ, J., PLESCH, G., KRÄTSMÁR-ŠMOGROVIČ, J., SVAJLENOVA, O. & KETTMANN, V. (1989). Proc. 12th Conf. Coordination Chemistry, Smolenice, Bratislava, 6-9 June 1989, pp. 349-354.
SIVÝ, P., VALACH, F., KOREŇ, B., MACÁŠKOVÁ, L., PAVELČÍK, F. & SIVÝ, J. (1989). *Acta Cryst.* C**45**, 1689.
ULICKÁ, L., PAVELČÍK, F. & HUML, K. (1987). *Acta Cryst.* C**43**, 2266-2268.
VRÁBEL, V., PAVELČÍK, F., KELLÖ, E., MIERTUŠ, S., KONEČNÝ, V. & LOKAJ, J. (1985). *Collect. Czech. Chem. Commun.* **50**, 1619-1628.
VRÁBEL, V., PAVELČÍK, F., KELLÖ, E., MIERTUŠ, S., KONEČNÝ, V. & LOKAJ, J. (1987). *Collect. Czech. Chem. Commun.* **52**, 696-706.
WONDRATSCHEK, H. (1989). In *International Tables for Crystallography*, Vol. A, pp. 728-730. Dordrecht: Kluwer Academic Publishers.
ZIMMERMANN, H. (1988). *Z. Kristallogr.* **183**, 113-122.

Acta Cryst. (1992). A**48**, 796-804

An Attempt to Describe One-Dimensional Incommensurate Composite Structure as Phason-Defected One-Dimensional Quasiperiodic Structure*

BY Y. F. CHENG AND F. H. LI

Institute of Physics, Chinese Academy of Sciences, Beijing 100080, *People's Republic of China, and Beijing Laboratory of Electron Microscopy, Chinese Academy of Sciences, Beijing* 100080, *People's Republic of China*

(*Received* 28 *December* 1990; *accepted* 25 *March* 1992)

Abstract

An incommensurate phase with one-dimensional (1D) incommensurate composite structure newly discovered in an Al-Cu-Fe alloy coexists with the structurally related commensurate phase. Both of them can be described as a phason-defected 1D fictitious quasicrystal. The 1D quasicrystal is obtained by cutting a six-dimensional (6D) crystal with physical space. With the increase of a particular linear phason strain, the section of the 6D crystal transfers firstly to the incommensurate phase and then to the commensurate phase.

1. Introduction

There are different types of incommensurate structures, for example, incommensurate modulated structure (de Wolff, 1974), incommensurate composite structure (Janner & Janssen, 1980) and quasiperiodic structure (Shechtman, Blech, Gratias & Cahn 1984). They can easily be distinguished one from another by means of diffraction data. The diffraction peaks of an incommensurate modulated structure can be divided into two groups: main peaks and satellite peaks. The main peaks form a periodic lattice that corresponds to the average structure and each main peak is accompanied by satellite peaks. The incommensurate composite structure consists of two or more substructures. Each of them gives an independent set of periodic diffraction peaks to form the major reflections. The minor reflections originate from the mutual interaction among different substructures. In this sense, both incommensurate modulated structures and incommensurate composite structures are to some extent related to three-dimensional (3D) periodicity. The quasicrystal possesses quasiperiodicity in both real and reciprocal spaces that is not related to 3D periodicity (Schechtman *et al.*, 1984). Thus far, the incommensurate modulated structure, the incommensurate composite structure and the quasicrystal structure are recognized as completely different incommensurate structures and no information about the structural relationship among them has been

* This project is supported by the National Natural Science Foundation of China.

0108-7673/92/060796-09$06.00

reported. However, they do have some similarity, for instance, in the incommensurate-commensurate phase transformation. A continuous incommensurate-commensurate phase transformation may occur for an incommensurate modulated structure during an increase of temperature and for an incommensurate composite crystal during a change of composition. An almost continuous quasicrystalline-crystalline phase transformation has also been observed and interpreted by introducing a particular linear phason strain (Li, Pan, Tao, Hui, Mai, Chen & Cai, 1989). In addition, some electron diffraction patterns (EDPs) of a newly discovered one-dimensional (1D) incommensurate composite structure (Cheng, Hui & Li, 1991) have some similarity with those of phason-defected quasicrystals. This led us to investigate the structural relationship between 1D incommensurate composite structure and 1D quasicrystal structure. In the following, firstly, the newly discovered 1D incommensurate composite structure (the σ' phase) and its coexisting commensurate structure (the σ phase) in the Al–Cu–Fe alloy will be introduced. Secondly, the relation to the fictitious 1D quasicrystal is discussed. Then the six-dimensional (6D) periodic structure that related to the σ phase, the σ' phase and the 1D quasicrystal is derived. Finally, it will be shown that both the σ and σ' phases can be treated as phason-defected 1D quasiperiodic structures.

2. The σ and σ' phases

The σ phase is a newly discovered tetragonal phase in rapidly quenched $Al_{77}Cu_{10}Fe_{13}$ and $Al_{73}Cu_{18}Fe_9$ alloys (Cheng *et al.*, 1991). The lattice parameters are $a_0 = 9.07$, $c_0 = 21.9$ Å and the approximate composition is $Al_{80}Cu_5Fe_{15}$. The space group, determined by combining conventional and convergent-beam electron diffraction, is $I4/mmm$. Fig. 1(a) gives a set of selected-area electron diffraction patterns (EDPs) taken from different zone axes covering an orientational triangle. The σ phase coexists with a 1D incommensurate composite phase (σ' phase) that also has point-group symmetry of $4/mmm$. In the EDPs for the σ' phase (Figs. 2a,b,c) the distance between two adjacent diffraction spots along the c^* direction does not remain constant. This indicates that the crystal structure is incommensurate and the incommensuration occurs along the fourfold axis. All diffraction spots can be indexed with four indices h, k, l_1, l_2. Hence, the σ' phase was determined as a 1D incommensurate composite crystal consisting of two interpenetrating substructures with sublattice parameters $a_1 = a_0$, $c_1 \simeq \frac{1}{7}c_0 = 3.14$ Å (substructure I) and $a_2 = 2^{-1/2}a_0$, $c_2 = 3.71$ Å (substructure II) respectively (Cheng *et al.*, 1991). However, the relation between Fig. 2(a) and the [100] zone-axis pattern in Fig. 1(a) is similar to the transformation from a phason-defected quasicrystal to an approximate crystal structure. An evident deviation of the former from the latter is that in Fig. 2(a) the diffraction spots are no longer aligned along straight lines running from bottom right to top left and from bottom left to top right. In addition, the deviation of the positions of spots in Fig. 2(a) from those of the [100] pattern in Fig. 1(a) is larger for weaker spots and *vice versa*. This is similar to the peak shift of a phason-defected quasicrystal (Lubensky, Socolar, Steinhardt, Bancel & Heiney, 1986; Bancel & Heiney, 1986; Socolar & Wright, 1987). Furthermore, the deviation, which is different for different grains or for different areas inside a grain, is similar to that in a phason-defected quasicrystal (Li *et al.*, 1989).

3. From 1D quasicrystal to 6D crystal

3.1. *The link to the* 1*D quasicrystal*

The above argument leads to an assumption that the transformation from the σ' phase to the σ phase may be caused by the action of a particular linear phason strain that acts along the fourfold axis and does not change the symmetry of the structure. In such a case the zero-phason state should be a 1D quasicrystal whose point-group symmetry is still $4/mmm$, where the periodicity along the fourfold axis breaks down and is replaced by a quasiperiodicity, which may, for instance, obey the golden ratio τ $[\tau = (1+5^{1/2})/2]$. Under the action of a particular linear phason strain this fictitious 1D quasicrystal would transform to the σ' phase and then to the σ phase. In general, a 1D quasicrystal can easily be obtained by cutting a four-dimensional (4D) periodic crystal. But in the present case one cannot expect to obtain a 1D quasicrystal that is related to the σ' and σ phases in a 4D crystal. In the following it will be shown that such a 1D quasicrystal can be obtained by cutting a 6D crystal.

3.2. *Derivation of* 6*D periodic structure*

A Cartesian coordinate system is used in the physical space $E_\parallel$ with unit vectors $\mathbf{a}_\parallel^x$, $\mathbf{a}_\parallel^y$ and $\mathbf{a}_\parallel^z$ along the coordinate axes X, Y and Z respectively. From Feng *et al.* (1990), a set of six bases $\mathbf{b}_\parallel^i$ ($i = 1$ to 6) may be constructed in this space to describe the 1D quasicrystal and which can be related to the Cartesian coordinate system as follows:

$$\begin{aligned} \mathbf{b}_\parallel^1 &= (a_0/3)(1,0,0), & \mathbf{b}_\parallel^4 &= (a_0/3)(1,1,0), \\ \mathbf{b}_\parallel^2 &= (a_0/3)(0,1,0), & \mathbf{b}_\parallel^5 &= (a_0/3)(-1,1,0), \\ \mathbf{b}_\parallel^3 &= a_0(0,0,-A), & \mathbf{b}_\parallel^6 &= a_0(0,0,A\tau^2). \end{aligned} \qquad (1)$$

With the six bases constructed here, the generators of the point group $4/mmm$ {E, 4[001], m(100),

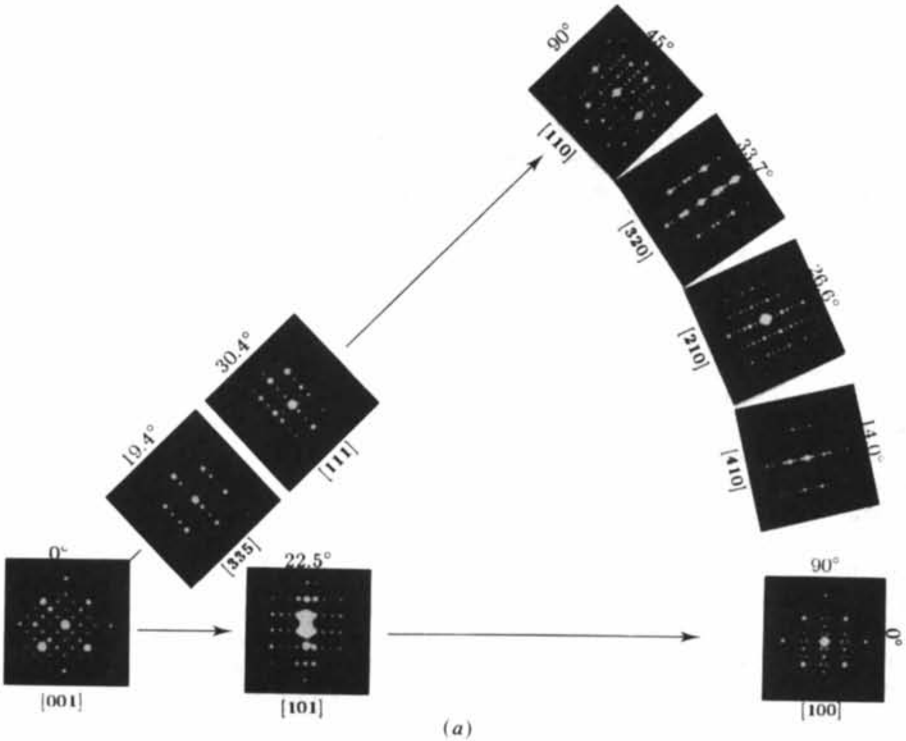

(a)

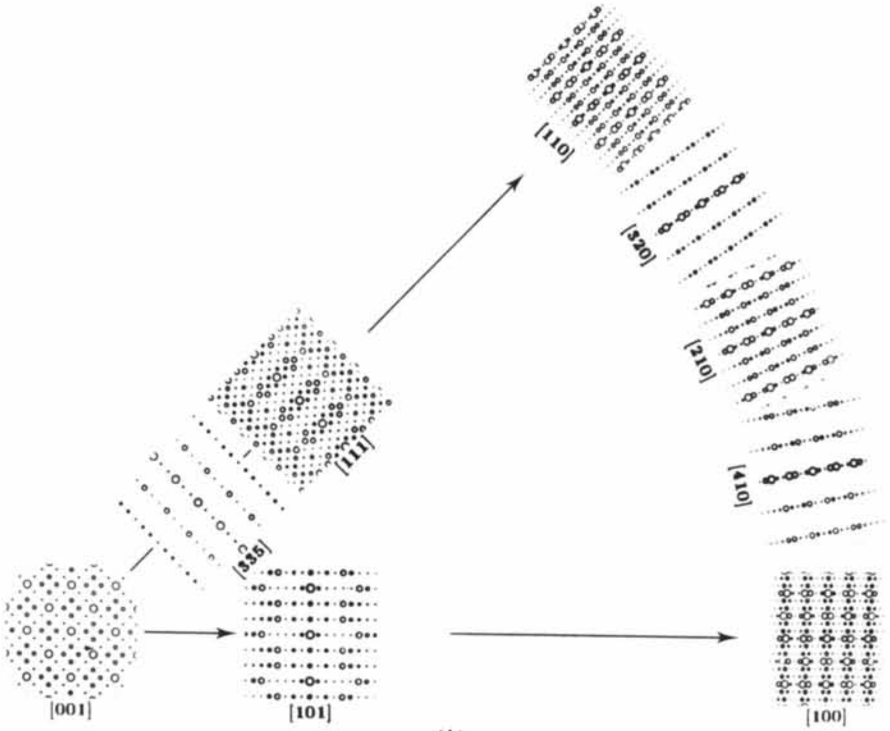

(b)

Fig. 1. (a) A set of EDPs of the commensurate σ phase taken along different zone axes covering an orientational triangle. (b) A set of simulated EDPs of commensurate σ phase, which correspond to the zone axes in (a). The calculations are based on the 1D phason-defected quasicrystal with $\alpha = -0.236$.

$m(001)\}$ are represented by the matrices

$$\{4[001]\} = \begin{pmatrix} 0 & 1 & 0 & 0 & 0 & 0 \\ -1 & 0 & 0 & 0 & 0 & 0 \\ 0 & 0 & 1 & 0 & 0 & 0 \\ 0 & 0 & 0 & 0 & 1 & 0 \\ 0 & 0 & 0 & -1 & 0 & 0 \\ 0 & 0 & 0 & 0 & 0 & 1 \end{pmatrix},$$

$$\{m(100)\} = \begin{pmatrix} 1 & 0 & 0 & 0 & 0 & 0 \\ 0 & -1 & 0 & 0 & 0 & 0 \\ 0 & 0 & 1 & 0 & 0 & 0 \\ 0 & 0 & 0 & 0 & -1 & 0 \\ 0 & 0 & 0 & -1 & 0 & 0 \\ 0 & 0 & 0 & 0 & 0 & 1 \end{pmatrix}, \qquad (2)$$

$$\{m(001)\} = \begin{pmatrix} 1 & 0 & 0 & 0 & 0 & 0 \\ 0 & 1 & 0 & 0 & 0 & 0 \\ 0 & 0 & -1 & 0 & 0 & 0 \\ 0 & 0 & 0 & 1 & 0 & 0 \\ 0 & 0 & 0 & 0 & 1 & 0 \\ 0 & 0 & 0 & 0 & 0 & -1 \end{pmatrix}$$

and $\{E\}$ is a unit matrix. These matrices form a 6D representation of the point group $4/mmm$. Because these matrices are quasidiagonalized, the 6D representation space could be decomposed into two orthogonal 3D subspaces. One is $E_\parallel$ and another is the pseudospace $E_\perp$. A Cartesian coordinate system is also used in $E_\perp$ with unit vectors $\mathbf{a}_\perp^x$, $\mathbf{a}_\perp^y$ and $\mathbf{a}_\perp^z$ along the axes $X_\perp$, $Y_\perp$ and $Z_\perp$ respectively. By combination of the Cartesian coordinate system in both $E_\parallel$ and $E_\perp$, an orthogonal coordinate system in 6D space can be obtained with the unit vectors $\mathbf{a}_\parallel^x$, $\mathbf{a}_\parallel^y$, $\mathbf{a}_\parallel^z$, $\mathbf{a}_\perp^x$, $\mathbf{a}_\perp^y$ and $\mathbf{a}_\perp^z$. In 6D space, a periodic lattice can be constructed such that the components of its bases $\mathbf{B}_i$ ($i = 1$ to 6) in the physical space $E_\parallel$ are coincident with $\mathbf{b}_\parallel^i$ mentioned above, while in pseudospace the bases $b_\perp^i$ are in the form

$$\begin{aligned} \mathbf{b}_\perp^1 &= (a_0/3)(-1, 1, 0), & \mathbf{b}_\perp^4 &= (a_0/3)(1, 0, 0), \\ \mathbf{b}_\perp^2 &= (a_0/3)(-1, -1, 0), & \mathbf{b}_\perp^5 &= (a_0/3)(0, 1, 0), \\ \mathbf{b}_\perp^3 &= a_0(0, 0, 2^{1/2}A\tau^3), & \mathbf{b}_\perp^6 &= a_0(0, 0, -2^{1/2}A\tau). \end{aligned} \qquad (3)$$

In this way, a simple form of the 6D periodic lattice that can be related to the σ' and σ phases as shown

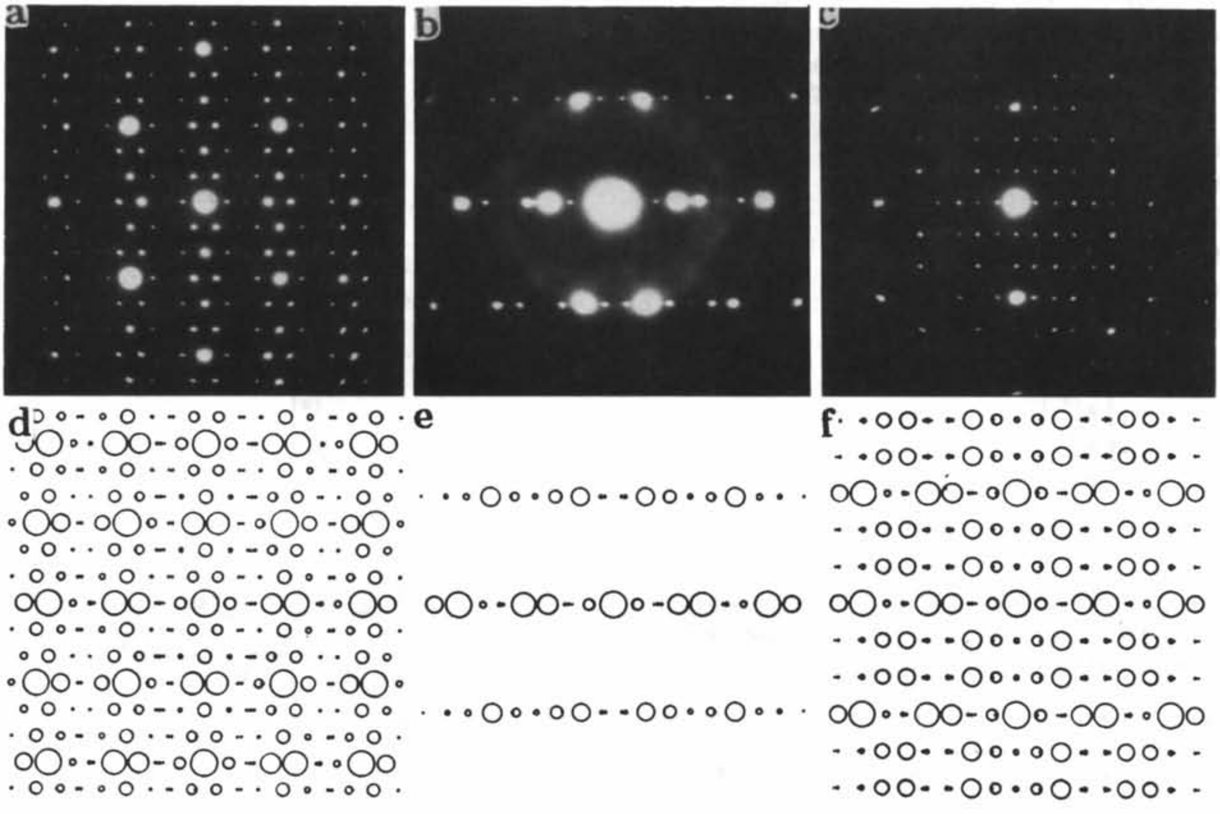

Fig. 2. A set of EDPs of the incommensurate σ' phase taken along (a) [100], (b) [410] and (c) [110] and the corresponding simulated patterns (d), (e) and (f) calculated with $\sigma = -0.2$.

later has been obtained with its bases written as

$$\begin{pmatrix}\mathbf{B}_1\\ \mathbf{B}_2\\ \mathbf{B}_3\\ \mathbf{B}_4\\ \mathbf{B}_5\\ \mathbf{B}_6\end{pmatrix} = \frac{a_0}{3}\begin{pmatrix} 1 & 0 & 0 & -1 & 1 & 0 & \mathbf{a}_\parallel^x\\ 0 & 1 & 0 & -1 & -1 & 0 & \mathbf{a}_\parallel^y\\ 0 & 0 & -3A & 0 & 0 & 3\times 2^{1/2}A\tau^3 & \mathbf{a}_\parallel^z\\ 1 & 1 & 0 & 1 & 0 & 0 & \mathbf{a}_\perp^x\\ -1 & 1 & 0 & 0 & 1 & 0 & \mathbf{a}_\perp^y\\ 0 & 0 & 3A\tau^2 & 0 & 0 & -3\times 2^{1/2}A\tau & \mathbf{a}_\perp^z \end{pmatrix} = P\begin{pmatrix}\mathbf{a}_\parallel^x\\ \mathbf{a}_\parallel^y\\ \mathbf{a}_\parallel^z\\ \mathbf{a}_\perp^x\\ \mathbf{a}_\perp^y\\ \mathbf{a}_\perp^z\end{pmatrix}. \quad (4)$$

The 6D periodic lattice is represented by the lattice function $L_0(\mathbf{r}_\parallel, \mathbf{r}_\parallel)$, which consists of δ functions with their centers at the nodes $\mathbf{R}=(\mathbf{R}_\parallel, \mathbf{R}_\parallel)$. Based on the reciprocal principle $\mathbf{B}_i\cdot\mathbf{B}_j^*=\delta_{ij}$, the bases of the 6D reciprocal lattice can be written in the form of their components in the reciprocal subspaces $E_\parallel^*$ and $E_\perp^*$:

$$\begin{pmatrix}\mathbf{B}_1^*\\ \mathbf{B}_2^*\\ \mathbf{B}_3^*\\ \mathbf{B}_4^*\\ \mathbf{B}_5^*\\ \mathbf{B}_6^*\end{pmatrix} = \frac{1}{a_0}\begin{pmatrix} 1 & 0 & 0 & -1 & 1 & 0 & \mathbf{a}_\parallel^{x*}\\ 0 & 1 & 0 & -1 & -1 & 0 & \mathbf{a}_\parallel^{y*}\\ 0 & 0 & p\tau & 0 & 0 & 2^{-1/2}p\tau^2 & \mathbf{a}_\parallel^{z*}\\ 1 & 1 & 0 & 1 & 0 & 0 & \mathbf{a}_\perp^{x*}\\ -1 & 1 & 0 & 0 & 1 & 0 & \mathbf{a}_\perp^{y*}\\ 0 & 0 & p\tau^3 & 0 & 0 & 2^{-1/2}p & \mathbf{a}_\perp^{z*} \end{pmatrix} = P^*\begin{pmatrix}\mathbf{a}_\parallel^{x*}\\ \mathbf{a}_\parallel^{y*}\\ \mathbf{a}_\parallel^{z*}\\ \mathbf{a}_\perp^{x*}\\ \mathbf{a}_\perp^{y*}\\ \mathbf{a}_\perp^{z*}\end{pmatrix}. \quad (5)$$

Here, $P^*=(P^{-1})^T$ (where T denotes the transpose) and $p=1/[A\tau^2(\tau^2+1)]$. There are six bases in both reciprocal subspaces $E_\parallel^*$ and $E_\perp^*$. They are

$$\begin{aligned} &\mathbf{b}_\parallel^{1*}=(1/a_0)(1,0,0), && \mathbf{b}_\parallel^{4*}=(1/a_0)(1,1,0),\\ &\mathbf{b}_\parallel^{2*}=(1/a_0)(0,1,0), && \mathbf{b}_\parallel^{5*}=(1/a_0)(-1,1,0),\\ &\mathbf{b}_\parallel^{3*}=(1/a_0)(0,0,p\tau), && \mathbf{b}_\parallel^{6*}=(1/a_0)(0,0,p\tau^3) \end{aligned} \quad (6a)$$

and

$$\begin{aligned} &\mathbf{b}_\perp^{1*}=(1/a_0)(-1,1,0), && \mathbf{b}_\perp^{4*}=(1/a_0)(1,0,0),\\ &\mathbf{b}_\perp^{2*}=(1/a_0)(-1,-1,0), && \mathbf{b}_\perp^{5*}=(1/a_0)(0,1,0),\\ &\mathbf{b}_\perp^{3*}=(1/a_0)(0,0,2^{-1/2}p\tau^2), && \\ & && \mathbf{b}_\perp^{6*}=(1/a_0)(0,0,2^{-1/2}p), \end{aligned} \quad (6b)$$

where $a_0=9.07$ Å is the lattice parameter of the σ and σ' phases along the [100] direction and $p=a_0/c_0=0.414$. Fig. 3 shows the configurations of bases $\mathbf{b}_\parallel^{i*}$ and $\mathbf{b}_\perp^{i*}$ in $E_\parallel^*$ and $E_\perp^*$ respectively.

The 6D periodic structure could be described by the function

$$\rho_0(\mathbf{r}_\parallel, \mathbf{r}_\perp)=\delta(\mathbf{r}_\perp)*L_0(\mathbf{r}_\parallel,\mathbf{r}_\perp)*\varphi_0(\mathbf{r}_\parallel,\mathbf{r}_\perp), \quad (7)$$

where all lattice nodes have a definite shape along $E_\perp$ described by the window function $S(\mathbf{r}_\perp)$ and the atomic decoration in the 6D unit cell is described by the function $\varphi_0(\mathbf{r}_\parallel, \mathbf{r}_\perp)$. The shape of hyperatoms in the pseudospace $E_\perp$ is also described by the function $S(\mathbf{r}_\perp)$.

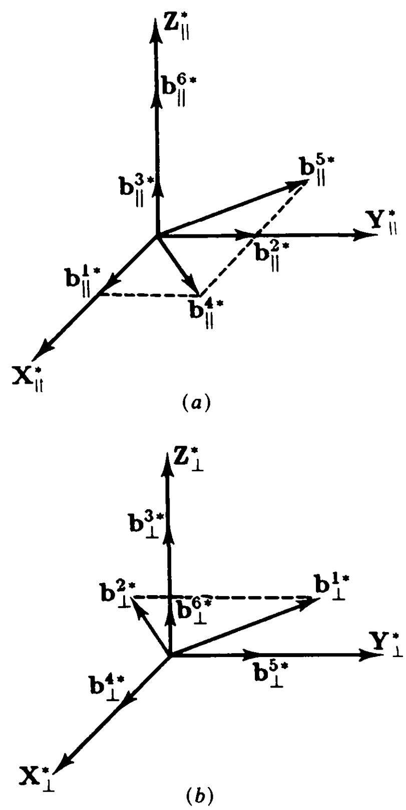

Fig. 3. The configuration of six bases (a) $\mathbf{b}_\parallel^{i*}$ and $\mathbf{b}_\perp^{i*}$ in the reciprocal spaces $E_\parallel^*$ and $E_\perp^*$, respectively.

3.3. *Cutting the 6D periodic structure*

The cut method was first proposed by de Wolff (1977) for describing incommensurate modulated structure. After the discovery of quasicrystals (Shechtman *et al.*, 1984) it has been widely used for describing quasicrystals (Kramer & Neri, 1984; Kalugin, Kitaev & Levitov, 1985; Duneau & Katz, 1985; Elser, 1986). The phason-defected quasicrystal structure formulation given by Li & Cheng (1990) was also based on the cut description.

The section of the 6D periodic structure described by (7) that is cut by the 3D physical space $E_\parallel$ gives the 3D structure with point-group symmetry of $4/mmm$ and 1D quasiperiodicity along its fourfold axis. The Fourier transformation of this 1D quasiperiodic structure in the 3D physical space can be obtained by projecting the 6D reciprocal lattice onto the physical reciprocal space $E_\parallel^*$. The projected reciprocal vectors $\mathbf{G}_\parallel$ in the reciprocal physical space $E_\parallel^*$ can be obtained by using the formula

$$\mathbf{G}_\parallel=\begin{pmatrix}G_\parallel^x\\G_\parallel^y\\G_\parallel^z\end{pmatrix}=\frac{1}{a_0}\begin{pmatrix}1&0&0&1&-1&0\\0&1&0&1&1&0\\0&0&p\tau&0&0&p\tau^3\end{pmatrix}\begin{pmatrix}n_1\\n_2\\n_3\\n_4\\n_5\\n_6\end{pmatrix}=\frac{1}{a_0}P_\parallel^*\begin{pmatrix}n_1\\n_2\\n_3\\n_4\\n_5\\n_6\end{pmatrix}, \tag{8}$$

where $P_\parallel^*$ is the projection matrix. Thus every diffraction spot can be indexed by six indices (n_1, n_2, n_3, n_4, n_5, n_6), which are constrained by $n_1+n_2+n_3=$ even and $n_4+n_5+n_6=$ even. The structure factors of the 1D quasiperiodic structure in $E_\parallel$ is expressed as (Li & Wang, 1988; Yamamoto & Hiraga, 1988; Li & Cheng, 1990):

$$\mathbf{F}_{\mathbf{G}_\parallel}=s(\mathbf{G}_\perp)\mathbf{F}_0(\mathbf{G}_\parallel,\mathbf{G}_\perp), \tag{9}$$

where $\mathbf{F}_0$ denotes the structure factor of the 6D structure and is equal to the Fourier transform of the function $\varphi(\mathbf{r}_\parallel,\mathbf{r}_\perp)$; $s(\mathbf{G}_\perp)$ is the Fourier transform of the shape function $S(\mathbf{r}_\perp)$ of lattice nodes and the hyperatoms. $\mathbf{G}_\perp$ denotes the projection of 6D reciprocal vectors onto pseudospace $E_\perp^*$,

$$\mathbf{G}_\perp=\begin{pmatrix}G_\perp^x\\G_\perp^y\\G_\perp^z\end{pmatrix}=\frac{1}{a_0}\begin{pmatrix}-1&-1&0&1&0&0\\1&-1&0&0&1&0\\0&0&2^{-1/2}p\tau^2&0&0&2^{-1/2}p\end{pmatrix}\begin{pmatrix}n_1\\n_2\\n_3\\n_4\\n_5\\n_6\end{pmatrix}=\frac{1}{a_0}P_\perp^*\begin{pmatrix}n_1\\n_2\\n_3\\n_4\\n_5\\n_6\end{pmatrix}, \tag{10}$$

where $P_\perp^*$ is the projection matrix.

3.4. *Determination of the size of the hyperatoms*

For simplicity, the shape of hyperatoms in pseudospace is assumed to approximate a sphere with radius r_c, which is an adjustable parameter and can be determined by fitting the EDPs of the 1D quasicrystal to those of the σ phase. Since the structures of the σ and σ' phases are unknown, the atomic decoration is ignored in the following.

Fig. 4 shows the calculated EDPs of the fictitious 1D quasicrystal for the [001], [100] and [110] zone axes, respectively. In the EDP of the [001] zone axis (Fig. 4*a*), the pattern is periodic and has fourfold symmetry. In the EDPs of the [100] and [110] zone axes (Figs. 4*b*,*c*), the arrangement of diffraction spots obeys the golden ratio along the horizontal (direction parallel to the fourfold axis), but shows periodicity along the vertical direction. The calculated patterns confirm that the constructed 1D quasicrystal is really a tetragonal 1D quasicrystal with point group $4/mmm$.

4. Description of σ' and σ phases as phason-defected 1D quasicrystals

The linear phason strain in a quasicrystal is described by a second-rank tensor, which can be expressed as a 3×3 matrix. In the present case, the action of the linear phason strain is along the fourfold axis and the strain strength is uniform everywhere. Therefore, the phason-strain matrix is expressed as

$$M=2^{1/2}\begin{pmatrix}0&0&0\\0&0&0\\0&0&\alpha\end{pmatrix}. \tag{11}$$

By the action of this linear phason strain, the diffraction spots of the 1D quasicrystal are displaced to form new reciprocal vectors $\mathbf{G}'_{\parallel}$ in $E^*_{\parallel}$ (Lubensky *et al.*, 1986):

$$\mathbf{G}'_{\parallel}=\mathbf{G}_{\parallel}+M\mathbf{G}_{\perp}$$

$$=\frac{1}{a_0}\begin{pmatrix}1 & 0 & 0 & 1 & -1 & 0\\ 0 & 1 & 0 & 1 & 1 & 0\\ 0 & 0 & p\tau(1+\tau\alpha) & 0 & 0 & p(\tau^3+\alpha)\end{pmatrix}\times\begin{pmatrix}n_1\\ n_2\\ n_3\\ n_4\\ n_5\\ n_6\end{pmatrix}. \qquad (12)$$

The phason-defected bases in $E^*_{\parallel}$ are now represented by

$$\mathbf{b}^{1*\prime}_{\parallel}=(1/a_0)(1,0,0), \qquad \mathbf{b}^{4*\prime}_{\parallel}=(1/a_0)(1,1,0),$$
$$\mathbf{b}^{2*\prime}_{\parallel}=(1/a_0)(0,1,0), \qquad \mathbf{b}^{5*\prime}_{\parallel}=(1/a_0)(-1,1,0),$$
$$\mathbf{b}^{3*\prime}_{\parallel}=(1/a_0)(0,0,q), \qquad \mathbf{b}^{6*\prime}_{\parallel}=(1/a_0)(0,0,4r), \qquad (13)$$

where $q=p\tau(1+\tau\alpha)$ and $r=p(\tau^3+\alpha)/4$.

When $\alpha=-0.2$, the 1D quasicrystal transforms into the 1D incommensurate σ' phase. Figs. 2(d), (e) and (f) are the simulated EDPs of the phason-defected 1D quasicrystal with $\alpha=-0.2$ for the [100], [410] and [110] zone axes respectively. They are generally in agreement with those of the σ' phase (Figs. 2a,b,c). When $\alpha=-0.236$, q/r becomes a rational number (=1) and the 1D quasicrystal transforms into the commensurate tetragonal σ phase. The simulated EDPs of the 1D phason-defected quasicrystal with $\alpha=-0.236$ of different zone axes are shown in Fig. 1(b). They are in agreement with those of the σ phase (Fig. 1a).

The agreement of simulated EDPs of the 1D phason-defected quasicrystal with those of the σ' and σ phases indicates that the structure of the commensurate σ phase and its related incommensurate σ' phase can be described as the phason-defected 1D quasicrystal. In such a case, the incommensurate σ' phase is an intermediate state between the 1D quasicrystal and the σ phase, but the σ' phase is closer to the σ phase than to the artificial 1D quasicrystal.

Because all the simulated EDPs are obtained by ignoring the atomic decoration, it is expected that the agreement of simulated EDPs with the experimental EDPs will become closer when the atomic decoration is taken into consideration. For instance, the diffraction-spot size in the simulated EDPs will decrease with the increase of the spatial frequency so that the simulated EDPs will be a better fit to the experimental ones.

5. Discussion and concluding remarks

In the constructed 6D lattice, with the exception of bases $\mathbf{B}_3$ and $\mathbf{B}_6$, the bases are perpendicular to each other and have the same length. Bases $\mathbf{B}_3$ and $\mathbf{B}_6$ are not perpendicular to each other but they are perpendicular to all other bases. Their lengths differ from each other and also from the other four bases. The case for the 6D reciprocal lattice is exactly the same. The existence of diffraction conditions $n_1+n_2+n_3=$ even and $n_4+n_5+n_6=$ even indicated that the 6D periodic lattice with bases $\mathbf{B}_i$ is not a simple lattice. There are four lattice nodes $[(0,0,0,0,0,0)$, $(\frac{1}{2},\frac{1}{2},\frac{1}{2},0,0,0)$, $(0,0,0,\frac{1}{2},\frac{1}{2},\frac{1}{2})$ and $(\frac{1}{2},\frac{1}{2},\frac{1}{2},\frac{1}{2},\frac{1}{2},\frac{1}{2})]$ in one unit cell.

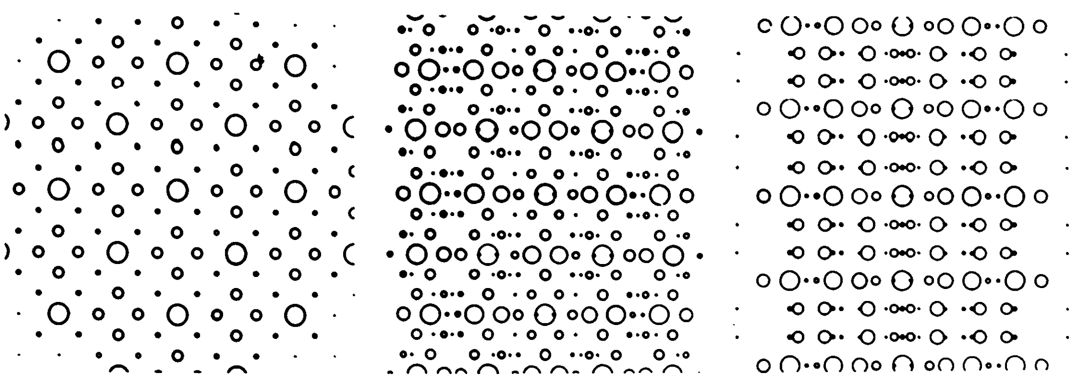

(a) (b) (c)

Fig. 4. The calculated EDPs of a 1D fictitious tetragonal quasicrystal for the (a) [001], (b) [100] and (c) [110] zone axes.

Another set of 6D bases in both real and reciprocal 6D space can be selected:

$$\begin{pmatrix} \mathbf{B}'_1 \\ \mathbf{B}'_2 \\ \mathbf{B}'_3 \\ \mathbf{B}'_4 \\ \mathbf{B}'_5 \\ \mathbf{B}'_6 \end{pmatrix} = \frac{a_0}{6}\begin{pmatrix} 1 & -1 & -3A & 0 & 2 & 3\times 2^{1/2}A\tau^2 \\ 1 & -1 & 3A & 0 & 2 & -3\times 2^{1/2}A\tau^2 \\ 0 & 2 & 0 & -2 & -2 & 0 \\ 2 & 0 & 3A\tau^2 & 1 & -1 & -3\times 2^{1/2}A\tau \\ 2 & 0 & -3A\tau^2 & 1 & -1 & 3\times 2^{1/2}A\tau \\ -2 & 2 & 0 & 0 & 2 & 0 \end{pmatrix} \times \begin{pmatrix} \mathbf{a}^x_\parallel \\ \mathbf{a}^y_\parallel \\ \mathbf{a}^z_\parallel \\ \mathbf{a}^x_\perp \\ \mathbf{a}^y_\perp \\ \mathbf{a}^z_\perp \end{pmatrix} \quad (14a)$$

and

$$\begin{pmatrix} \mathbf{B}'^*_1 \\ \mathbf{B}'^*_2 \\ \mathbf{B}'^*_3 \\ \mathbf{B}'^*_4 \\ \mathbf{B}'^*_5 \\ \mathbf{B}'^*_6 \end{pmatrix} = \frac{1}{a_0}\begin{pmatrix} 1 & 0 & p\tau & -1 & 1 & 2^{-1/2}p\tau^2 \\ 1 & 0 & -p\tau & -1 & 1 & -2^{-1/2}p\tau^2 \\ 1 & 1 & 0 & -2 & 0 & 0 \\ 1 & 1 & p\tau^3 & 1 & 0 & 2^{-1/2}p \\ 1 & 1 & -p\tau^3 & 1 & 0 & -2^{1/2}p \\ 0 & 2 & 0 & 1 & 1 & 0 \end{pmatrix} \times \begin{pmatrix} \mathbf{a}^x_\parallel \\ \mathbf{a}^y_\parallel \\ \mathbf{a}^z_\parallel \\ \mathbf{a}^x_\perp \\ \mathbf{a}^y_\perp \\ \mathbf{a}^z_\perp \end{pmatrix}. \quad (14b)$$

Fig. 5 gives the configuration of the components of $\mathbf{B}'^*_i$ ($i=1$ to 6) in physical and pseudospaces, respectively. Based on this set of bases, for which there is no extinction condition, the simulated EDPs give the same results as those with the first set of bases and diffraction condition. This indicates that the lattice with bases $\mathbf{B}'_i$ is equivalent to that with bases $\mathbf{B}_i$ but the former is a simple lattice. The bases $\mathbf{B}'_i$ form a unit cell with lower symmetry than that formed by $\mathbf{B}_i$.

Among the six bases in physical space $E^*_\parallel$, only four bases are independent for the case of the 1D incommensurate structure (σ'). A system of four bases could be presented for this case:

$$\begin{aligned} \mathbf{a}^*_1 &= (1/a_0)(1,0,0) \\ \mathbf{a}^*_2 &= (1/a_0)(0,1,0) \\ \mathbf{a}^*_3 &= (1/a_0)(0,0,8r-q) \\ \mathbf{a}^*_4 &= (1/a_0)(0,0,4r-q). \end{aligned} \quad (15)$$

All diffraction spots of the σ' phase can thus be indexed by four indices (hkl_1l_2). The relation between $\mathbf{b}^{i*'}_\parallel$ ($i=1$ to 6) and $\mathbf{a}^*_j$ ($j=1$ to 4) is

$$\begin{pmatrix} \mathbf{b}^{1*'}_\parallel \\ \mathbf{b}^{2*'}_\parallel \\ \mathbf{b}^{3*'}_\parallel \\ \mathbf{b}^{4*'}_\parallel \\ \mathbf{b}^{5*'}_\parallel \\ \mathbf{b}^{6*'}_\parallel \end{pmatrix} = \begin{pmatrix} 1 & 0 & 0 & 0 \\ 0 & 1 & 0 & 0 \\ 0 & 0 & 1 & -2 \\ 1 & 1 & 0 & 0 \\ -1 & 1 & 0 & 0 \\ 0 & 0 & 1 & -1 \end{pmatrix} \begin{pmatrix} \mathbf{a}^*_1 \\ \mathbf{a}^*_2 \\ \mathbf{a}^*_3 \\ \mathbf{a}^*_4 \end{pmatrix}, \quad (16)$$

the relation between the indices (hkl_1l_2) and

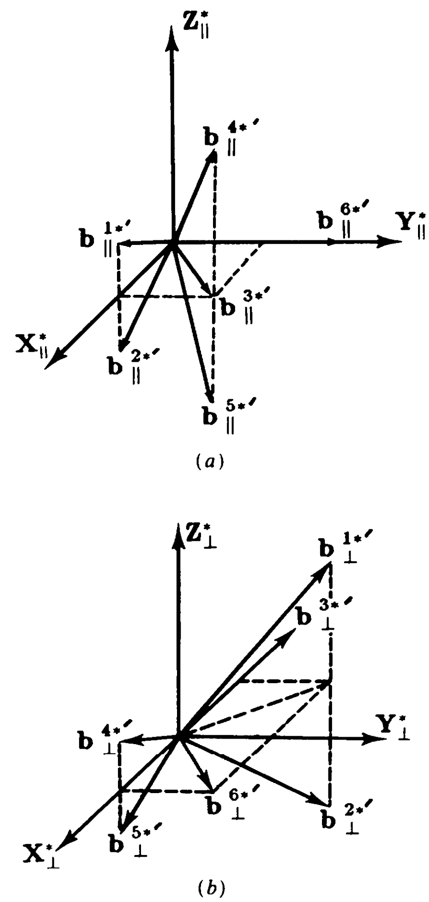

Fig. 5. Another set of bases (a) $\mathbf{b}^{i*'}_\parallel$ and (b) $\mathbf{b}^{i*'}_\perp$ in $E^*_\parallel$ and $E^*_\perp$, respectively.

$(n_1n_2n_3n_4n_5n_6)$ can be written as

$$\begin{aligned} h &= n_1 + n_4 - n_5 \\ k &= n_2 + n_4 + n_5 \\ l_1 &= n_3 + n_6 \\ l_2 &= -2n_3 - n_6. \end{aligned} \tag{17}$$

Previously the diffraction spots of the σ' phase were indexed on the bases of the incommensurate composite structure (Cheng *et al.*, 1991). After carefully analyzing the simulated and experimental EDPs of the σ' phase, the sublattice parameter of substructure II along the c direction should be doubled to $c_2 = 7.42$ Å. Thus, the four indices hkl_1l_2 based on a phason-defected 1D quasicrystal are coincident with those based on the 1D incommensurate composite structure. This confirms once again that the description proposed in the present paper is equivalent to the regular description.

In principal, such a description is generally applicable for all 1D incommensurate composite crystals.

As a conclusion, the incommensurate composite σ' phase is described as the intermediate state between a fictitious 1D tetragonal quasicrystal and the commensurate σ phase. In other words, the incommensurate σ' phase and commensurate σ phase can be treated as a phason-defected 1D quasicrystal although the 1D quasicrystal is fictitious and has not been found in the Al-Cu-Fe alloy thus far. This implies that the incommensurate composite structure that shows two independent periodicities along the same direction may have some inherent relation with quasiperiodicity.

YFC thanks Professor Renhui Wang and Dr J G Wen for useful discussions.

References

BANCEL, P. A. & HEINEY, P. A. (1986). *J. Phys. (Paris) Colloq.* **47**, 341.

CHENG, Y. F., HUI, M. J. & LI, F. H. (1991). *Philos. Mag. Lett.* **63**, 49-55.

DUNEAU, M. & KATZ, A. (1985). *Phys. Rev. Lett.* **54**, 2688-2691.

ELSER, V. (1986). *Acta Cryst.* A**42**, 36-43.

FENG, Y. C., LU, G., YE, H. Q., KUO, K. H., WITHER, R. L. & VAN TENDELOO, G. (1990). *J. Phys. Condens. Matter*, **2**, 9749-9755.

JANNER, A. & JANSSEN, T. (1980). *Acta Cryst.* A**36**, 408-415.

KALUGIN, A., KITAEV, A. & LEVITOV, L. (1985). *Pis'ma Zh. Eksp. Teor. Fiz.* **41**, 119-121.

KRAMER, P. & NERI, R. (1984). *Acta Cryst.* A**40**, 580-587.

LI, F. H. & CHENG, Y. F. (1990). *Acta Cryst.* A**46**, 146-149.

LI, F. H., PAN, G. Z., TAO, S. Z., HUI, M. J., MAI, Z. H., CHEN, X. S. & CAI, L. Y. (1989). *Philos. Mag.* B**59**, 535-542.

LI, F. H. & WANG, L. C. (1988). *J. Phys. C*, **21**, 495-503.

LUBENSKY, T. C., SOCOLAR, J. E. S., STEINHARDT, P. J., BANCEL, P. A. & HEINEY, P. A. (1986). *Phys. Rev. Lett.* **57**, 1440-1443.

SHECHTMAN, D., BLECH, I., GRATIAS, D. & CAHN, J. W. (1984). *Phys. Rev. Lett.* **53**, 1951-1954.

SOCOLAR, J. E. S. & WRIGHT, D. C. (1987). *Phys. Rev. Lett.* **59**, 221-224.

WOLFF, P. M. DE (1974). *Acta Cryst.* A**30**, 777-785.

WOLFF, P. M. DE (1977). *Acta Cryst.* A**33**, 493-497.

YAMAMOTO, A. & HIRAGA, K. (1988). *Phys. Rev. B*, **37**, 6207-6214.

Acta Cryst. (1992). A**48**, 804-819

Experimental Tests of the Statistical Dynamical Theory

BY JOCHEN R. SCHNEIDER AND ROLAND BOUCHARD

Hamburger Synchrotronstrahlungslabor (HASYLAB) at Deutsches Elektronen-Synchrotron (DESY), Notkestrasse 85, D-2000 Hamburg 52, Germany

AND HANS A. GRAF AND HISAO NAGASAWA*

Hahn-Meitner-Institut, Glienicker Strasse 100, D-1000 Berlin 39, Germany

(*Received 8 October* 1991; *accepted 1 April* 1992)

Abstract

A homogeneous distribution of SiO_2 precipitates in Czochralski-grown silicon containing different amounts of oxygen were produced by annealing the dislocation-free crystals at 1023 K. The resulting long-range strain field modifies the integrated reflecting power R of the Bragg reflections measured on an absolute scale with 316 keV γ-radiation. The thickness dependence of R has been modelled using the results of statistical dynamical theory. The assumption made in Kato's original theory, where the correlation length Γ for the wave-field amplitudes is proportional to the extinction length, has to be abandoned.

* Present address: Seikei University, Department of Economics, Kichijojikita-machi 3-3-1, Musashino-shi, Tokyo 180, Japan.

0108-7673/92/060804-16$06.00